J Neurophysiol
87: 1348–1362, 2002; 10.1152/jn.00582.2001.

Regulation of the Timing and Pattern of Action Potential Generation in Rat Subthalamic Neurons In Vitro by GABA-A IPSPs

M. D. BEVAN,[1,2] P. J. MAGILL,[2] N. E. HALLWORTH,[1] J. P. BOLAM,[2] AND C. J. WILSON[3]
[1]*Department of Anatomy and Neurobiology, University of Tennessee, Memphis, Tennessee 38163;* [2]*University of Oxford, Medical Research Council Anatomical Neuropharmacology Unit, Oxford OX1 3TH, United Kingdom; and* [3]*Division of Life Science, University of Texas, San Antonio, Texas 78294*

Received 16 July 2001; accepted in final form 2 November 2001

Bevan, M. D., P. J. Magill, N. E. Hallworth, J. P. Bolam, and C. J. Wilson. Regulation of the timing and pattern of action potential generation in rat subthalamic neurons in vitro by GABA-A IPSPs. *J Neurophysiol* 87: 1348–1362, 2002; 10.1152/jn.00582.2001. The regulation of activity in the subthalamic nucleus (STN) by GABAergic inhibition from the reciprocally connected globus pallidus (GP) plays an important role in normal movement and disorders of movement. To determine the precise manner in which GABAergic synaptic input, acting at A-type receptors, influences the firing of STN neurons, we recorded the response of STN neurons to GABA-A inhibitory postsynaptic potentials (IPSPs) that were evoked by supramaximal electrical stimulation of the internal capsule using the perforated-patch technique in slices at 37°C. The mean equilibrium potential of the GABA-A IPSP (EGABA-A IPSP) was −79.4 ± 7.0 mV. Single IPSPs disrupted the spontaneous oscillation that underlies rhythmic single-spike firing in STN neurons. As the magnitude of IPSPs increased, the effectiveness of prolonging the interspike interval was related more strongly to the phase of the oscillation at which the IPSP was evoked. Thus the largest IPSPs tended to reset the oscillatory cycle, whereas the smallest IPSPs tended to produce relatively phase-independent delays in firing. Multiple IPSPs were evoked at various frequencies and over different periods and their impact was studied on STN neurons held at different levels of polarization. Multiple IPSPs reduced and/or prevented action potential generation and/or produced sufficient hyperpolarization to activate a rebound depolarization, which generated a single spike or restored rhythmic spiking and/or generated a burst of activity. The pattern of IPSPs and the level of polarization of STN neurons were critical in determining the nature of the response. The duration of bursts varied from 20 ms to several hundred milliseconds, depending on the intrinsic rebound properties of the postsynaptic neuron. These data demonstrate that inhibitory input from the GP can produce a range of firing patterns in STN neurons, depending on the number and frequencies of IPSPs and the membrane properties and voltage of the postsynaptic neuron.

INTRODUCTION

Glutamatergic neurons of the subthalamic nucleus (STN) possess intrinsic membrane properties that are likely to contribute to their patterns of activity during normal movement and disordered movement (Beurrier et al. 1999, 2000; Bevan and Wilson 1999; Bevan et al. 2000; Nakanishi et al. 1987a; Overton and Greenfield 1995; Song et al. 2000). In vitro STN neurons discharge in a rhythmic single-spike pattern (Beurrier et al. 1999, 2000; Bevan and Wilson 1999; Bevan et al. 2000; Overton and Greenfield 1995). This activity is generated by an intrinsic oscillation, the principal pacemaker for which is the persistent sodium current (Beurrier et al. 2000; Bevan and Wilson 1999). This oscillation may, in part, underlie the tonic discharge of STN neurons in vivo (DeLong 1972; Georgopoulos et al. 1983; Matsumara et al. 1992; Wichmann et al. 1994) and the proposed function of the STN as a tonic driving force of neuronal activity in the basal ganglia of resting animals (Albin et al. 1989; Crossman 1989; DeLong 1990; Nakanishi et al. 1987b; Rinvik and Ottersen 1993; Smith and Parent 1988). In vitro STN neurons also discharge in high-frequency bursts on removal of hyperpolarizing current of sufficient amplitude (Beurrier et al. 1999, 2000; Bevan and Wilson 1999; Bevan et al. 2000; Nakanishi et al. 1987a; Overton and Greenfield 1995; Song et al. 2000). This rebound burst activity is generated, in part, by low-threshold calcium current that is inactivated during the oscillation but recovers from inactivation when STN neurons are hyperpolarized (Beurrier et al. 1999, 2000; Bevan and Wilson 1999; Bevan et al. 2000; Nakanishi et al. 1987a; Song et al. 2000). Since STN neurons may discharge in high-frequency bursts in an irregular manner during movement (DeLong 1972; DeLong et al. 1985; Georgopoulos et al. 1983; Matsumara et al. 1992; Wichmann et al. 1994), low-threshold calcium current may contribute to this pattern of activity if STN neurons are sufficiently hyperpolarized in vivo.

Subthalamic neurons may also discharge in bursts in a rhythmic manner that is phase-related to resting tremor in idiopathic (Magariños-Ascone et al. 2000; Magnin et al. 2000; Rodriguez et al. 1998) and experimental models (Bergman et al. 1994) of Parkinson's disease. It has been proposed (Plenz and Kitai 1999) that STN neurons, and reciprocally connected GABAergic globus pallidus (GP) neurons, generate low-frequency oscillatory activity via a mechanism that is similar to that reported for sleep-related oscillations in the thalamus (see review by McCormick and Bal 1997, and references therein). One critical component of this network oscillation is the generation, by bursts of activity in GP neurons, of sufficient hyperpolarization in STN neurons to produce rebound burst firing (Plenz and Kitai 1999). Although it is well recognized that the GP is important for the regulation of STN neuronal

Address for reprint requests: M. D. Bevan, Dept. of Anatomy and Neurobiology, University of Tennessee, Rm. 515 Link, 855 Monroe Ave., Memphis, TN 38163 (E-mail: mbevan@utmem.edu).

The costs of publication of this article were defrayed in part by the payment of page charges. The article must therefore be hereby marked "*advertisement*" in accordance with 18 U.S.C. Section 1734 solely to indicate this fact.

activity in health and in disease [see the following reviews and papers referenced by Albin et al. (1989), Bergman et al. (1998), Chesselet and Delfs (1995), Crossman (1989), DeLong (1990), Levy et al. (1997), and Wichmann and DeLong (1996)], the precise manner in which GABAergic synaptic inputs, acting at A-type receptors, interact with the intrinsic oscillatory and rebound burst properties of STN neurons is unknown. A study, using the pressure-pulse application of GABA, implied that GABA-A inhibitory postsynaptic potentials (IPSPs) might hyperpolarize STN neurons to membrane potentials associated with the abolition of the oscillation and the recovery from inactivation of low-threshold calcium current (Bevan et al. 2000). Thus the principal objective of this study was to determine how GABA-A synaptic inputs interact with the intrinsic membrane properties of STN neurons and pattern their activity. Subthalamic neurons were recorded in brain slices using the perforated patch technique to maintain the natural regulation of ions in recorded neurons (Abe et al. 1994; Bevan et al. 2000; Kyrozis and Reichling 1995; Ulrich and Huguenard 1997). Electrical stimulation of the internal capsule rostral to the STN was employed to stimulate preferentially GABAergic axons from the GP (see review by Smith et al. 1998 and references therein). Actions of GABA at A-type receptors were isolated in the majority of experiments by the addition of a selective GABA-B receptor antagonist (Brugger et al. 1993) to the bathing media. The first aim was to determine the likely interaction of GABA-A synaptic inputs with the voltage-dependent properties of STN neurons by determining EGABA-A IPSP. The second aim was to study the impact of single GABA-A IPSPs on spontaneously active STN neurons by stimulating IPSPs at different points in the oscillatory cycle. The third aim was to compare the degree of hyperpolarization required for rebound burst firing with EGABA-A IPSP. The fourth aim was to characterize the impact of multiple IPSPs evoked at various frequencies and over different periods on STN neurons held at different levels of polarization to determine the conditions necessary for the generation of rebound burst activity.

METHODS

Slice preparation

Brain slices were prepared as described previously (Bevan and Wilson 1999). Thus 26 male Sprague-Dawley rats, 18–25 days old, were anesthetized deeply with ketamine (100 mg/kg; Willows Francis, Crawley, UK) and xylazine (10 mg/kg; Bayer, Germany) and perfused transcardially with 10–30 ml of ice-cold modified artificial cerebrospinal fluid (ACSF), which had been bubbled with 95% O_2-5% CO_2 and contained (in mM) 230 sucrose, 2.5 KCl, 1.25 Na_2HPO_4, 0.5 $CaCl_2$, 10 $MgSO_4$, and 10 glucose. Each brain was removed rapidly, blocked along the midline, and glued to the surface of a Perspex block, which was then mounted to the stage of a vibratome (VT 1000S; Leica, Nussloch, Germany) at an angle of 7° from the horizontal plane. Each hemisphere was immersed in ice-cold modified ACSF, and parasagittal slices containing the subthalamus were cut at a thickness of 300–350 μm. The slices were then transferred to a holding chamber, where they were submerged in ACSF, which was bubbled continuously with 95% O_2-5% CO_2, maintained at room temperature (25–30°C), and contained (in mM) 126 NaCl, 2.5 KCl, 1.25 Na_2HPO_4, 2 $CaCl_2$, 2 $MgSO_4$, and 10 glucose. Slices were held in this chamber for at least 1 h before recording.

Visualized recording

Individual slices were transferred to the recording chamber and perfused continuously (2–3 ml/min) with oxygenated ACSF at 35–37°C. A ×2.5 objective (Zeiss, Oberkochen, Germany) was used to locate the subthalamic nucleus within each slice. A ×63 water-immersion objective (Olympus, Tokyo) was used to examine STN neurons using infrared differential interference contrast video microscopy (Stuart et al. 1993) (Infrapatch Workstation, Luigs and Neumann, Ratingen, Germany). Somatic recordings were made using patch pipettes prepared from standard-wall borosilicate glass (Clarke, Reading, UK) with a P-2000 laser electrode puller (Sutter Instrument, Novaton, CA). Pipettes were filled with a solution containing (in mM) 106 K-$MeSO_4$, 25 KCl, 1 $MgCl_2.6H_2O$, 0.1 $CaCl_2.2H_2O$, 10 HEPES, 1 Na_4EGTA, 0.4 Na_2GTP, and 2 $Mg_{1.5}$ATP. The pH and osmolarity of the pipette solution were 7.3 and 290 mosmol, respectively. Gramicidin was added to the pipette solution at a concentration of 20–50 μg/ml less than 1 h before seal formation was attempted. The resistance of the filled pipettes ranged from 2 to 4 MΩ. Fast capacitative transients of the pipette were nulled on-line, but voltage errors due to series resistance were compensated off-line. Recordings were made in the perforated configuration and whole cell configurations using the fast current clamp mode of an EPC 9/2.C amplifier (HEKA, Lambrecht, Germany), which was operated using Pulse 8.5 software (HEKA). Signals were low-pass filtered at a frequency (1.7–33.3 kHz) that was one-third of the frequency of digitization (5–100 kHz). Junction potentials were not corrected during perforated patch recording because in contrast to the whole cell configuration, the concentrations of ions in the pipette are not necessarily equal to the concentration of ions in the recorded cell. As observed previously, voltages measured during perforated patch recording of STN neurons were similar to voltages measured in the whole cell configuration and were corrected for junction potential (see Bevan and Wilson 1999; Bevan et al. 2000). Thirty-one neurons were recorded in the perforated configuration, and in four cases, the whole cell configuration was established subsequently.

Electrical stimulation of GABA-A IPSPs

GABA-A IPSPs were elicited by bipolar electrical stimulation (A360 stimulus isolator; World Precision Instruments, Sarasota, FL) of the internal capsule rostral to the STN. The poles of stimulation were selected from a custom-built matrix of 20 stimulation electrodes (MX54CBWMB1; FHC, Maine, ME). The matrix was comprised of four rows of electrodes with five electrodes in each row. The tip of each electrode was separated from the tip of the nearest neighboring electrode by approximately 200 μm. The shank and tip of each electrode was approximately 125 μm and 10 μm diam, respectively. The impedance of each electrode was 50–100 kΩ. The two electrodes selected for stimulation were those that produced the largest IPSP in the absence of antidromic activation. Supramaximal stimulation was employed so that failure to stimulate GABAergic fibers would contribute little to the variability of the observed responses. Thus stimulation intensity (0.05–0.5 mA) was increased to generate the largest IPSP possible and then increased further by approximately 20%. The duration of stimulation was 0.1–0.2 ms. The generation of excitatory amino acid postsynaptic potentials (reviewed by Watkins 2000) by electrical stimulation of the internal capsule was prevented by the continuous bath-application of 50 μM (+)-2-amino-5-phosphonopentanoic acid (APV; Research Biochemicals, Natick, MA) and 20 μM 6,7-dinitroquinoxaline-2,3-dione (DNQX; Research Biochemicals). Multiple electrical stimulation of the internal capsule also elicited a small GABA-B IPSP in a minority of STN neurons (data not shown). To isolate the actions of GABA-A IPSPs on STN neurons, the selective GABA-B antagonist CGP 55845 (Brugger et al. 1993) (5 μM; Tocris Cookson, Bristol, UK) was bath-applied during all experiments involving multiple electrical stimulation of the internal

capsule and the majority of experiments involving single electrical stimulation. Furthermore, the selective GABA-A antagonist (+)-bicuculline (Curtis et al. 1970) (30 μM) was bath-applied in several cases to further verify that the effects of synaptic stimulation on action potential generation were due solely to GABA-A receptor activation.

Measurement of EGABA-A IPSP

The IPSP, evoked by supramaximal stimulation, was recorded in each neuron at various holding potentials in the current clamp mode (Fig. 1). GABA-A IPSPs were evoked at intervals of 10–15 s. Changes in holding potential were made 1 s before the stimulation of the IPSP to allow the membrane potential to reach a steady-state value. The equilibrium potential of the GABA-A IPSP was determined from the linear regression of plots of V_m against $IPSP_{mag}$ (Figs. 1 and 2; Origin 5, Microcal, Northampton, MA).

Measurement of the effects of GABA-A IPSPs on spontaneous action potential generation in STN neurons

Single GABA-A IPSPs were evoked in each neuron by supramaximal stimulation at intervals of 10–15 s, at various points in the oscillatory cycle underlying spontaneous rhythmic spiking (Figs. 2–4). Holding current was not applied to the postsynaptic neuron during these experiments. The influence of the IPSP on the oscillation was assessed from measurements that were made as described in Figs. 2–4.

Measurement of hyperpolarization required for rebound burst firing

Injections of varying amounts of hyperpolarizing current were made for 500 ms, and the maximum degree of hyperpolarization during current application was measured (Fig. 5). Rebound burst firing following the removal of current was defined as firing that was at least three times the rate of firing associated with spontaneous activity. The threshold for rebound burst firing was defined as the minimum value of peak hyperpolarization that preceded a rebound burst. The duration of rebound burst firing was defined as the longest period over which firing was at least three times the rate of spontaneous activity.

Measurement of the conditions necessary for the generation of rebound burst firing by GABA-A IPSPs

Multiple GABA-A IPSPs were evoked by electrical stimulation, and their impact was studied on STN neurons held at various levels of polarization. Steady-state levels of polarization of STN neurons were varied by the injection of constant current (−50 pA to 0 pA) at least 1 s prior to the generation of IPSPs. IPSPs were evoked using a variety of stimulation patterns. In one set of experiments, the interstimulus interval was fixed at 10 ms, and the number of stimuli was varied between 5 and 50. In another set of experiments, IPSPs were evoked over a period of approximately 500 ms, but the interstimulus interval and number of IPSPs were varied. Rebound burst firing that was evoked by synaptic potentials was measured as described for rebound burst firing evoked by current injection.

Data analysis

Data were analyzed using Axograph 4.0 (Axon Instruments, Union City, CA), Kaleidagraph 3.5 (Synergy, Reading, PA), Origin 5.0 (Microcal, Northampton, MA), Pulse-Tools 8.5 (HEKA), and Statview 5.0 (Cary, NC). Descriptive statistics refer to the mean ± SD. Frequency distributions of the experimental data were compared with normal distributions of similar means and SDs, which were constructed using random numbers generated by Statview, using the Kolmogorov-Smirnov (K-S) test. The means of unpaired and paired experimental datasets were compared with the Mann-Whitney *U* (M-WU) test and the Wilcoxon signed rank (WSR) test, respectively. Probability values of <0.05 were considered significant.

RESULTS

EGABA-A IPSP

Stable series resistances of 53.7 ± 24.6 MΩ ($n = 31$) were obtained 20–40 min after sealing, and a monosynaptic IPSP was elicited in STN neurons by bipolar electrical stimulation of the internal capsule. By evoking an IPSP at various levels of polarization and plotting V_m against $IPSP_{mag}$, it was determined that EGABA-A IPSP was −79.4 ± 7.0 mV ($n = 31$; Fig. 1). The frequency histogram of EGABA-A IPSP from this sample was not significantly different from a normal distribution (K-S test, $P > 0.99$). The whole cell configuration was established after perforated recording in four neurons. In these cases, EGABA-A IPSP shifted significantly to more positive values (EGABA-A IPSP = −80.1 ± 4.0 mV, perforated configuration; EGABA-A IPSP = −60.6 ± 6.0 mV, whole cell configuration; WSR test, $P = 0.0078$) as predicted by the Nernst equation (−42 mV) (Nernst 1888; see also Bevan et al. 2000). This observation confirms that EGABA-A IPSP was measured using the perforated configuration. Furthermore, the IPSP was due solely to actions at GABA-A receptors because it was blocked rapidly by the bath application of the selective GABA-A antagonist bicuculline (30 μM) in each case that the drug was applied ($n = 15$; Fig. 1*B*).

Impact of single GABA-A IPSPs on the spontaneous oscillation underlying rhythmic spiking in STN neurons

As EGABA-A IPSP was more hyperpolarized than the voltage range associated with the spontaneous oscillation, we predicted that a single GABA-A IPSP would delay the subsequent generation of an action potential if low-threshold calcium current and hyperpolarization-activated cationic current were not strongly deinactivated or activated by the IPSP, respectively. The nomenclature adopted for this part of the study is described in Fig. 2. Supramaximal stimulation generated IPSPs that ranged considerably in size (−10.2 ± 5.7 mV). In neurons in which the largest GABA-A IPSPs were evoked, IPSPs increased ISI_{ipsp} in a relatively powerful phase-dependent manner (Fig. 3, *A, B, E,* and *H*) and the times from the onset of synaptic stimulation to action potentials following IPSPs (*b*) were relatively similar over multiple trials, regardless of the phase at which IPSPs were evoked (Fig. 3, *A, B, E,* and *H*). Thus large IPSPs reset the phase of the oscillatory cycle so that action potentials following IPSPs occurred within a narrow time window. Large IPSPs appeared to reset the phase of the oscillation by driving the membrane potential to a narrow range of potentials, defined by the range of $IPSP_{peak}$ (Fig. 3, *A, B,* and *G*).

As GABA-A IPSPs decreased in size, the dependence of ISI_{ipsp} on the phase at which the IPSP was evoked decreased (Fig. 3, *C, D, F,* and *H*), and the dependence of *b* on the phase at which the IPSP was evoked became more apparent (Fig. 3, *C, D,* and *F*). Thus ISI_{ipsp} was similar when small IPSPs were evoked at different times in the oscillatory cycle and the time to action potential generation following the IPSP was longer when the IPSP occurred early in the cycle and shorter when the

IPSP occurred later in the cycle (Fig. 3, *C*, *D*, *F*, and *H*). In other words, small IPSPs increased ISI_{ipsp} in a relatively phase-independent manner and failed to reset consistently the phase of the oscillation so that action potentials that followed the IPSP were generated across a wide time window.

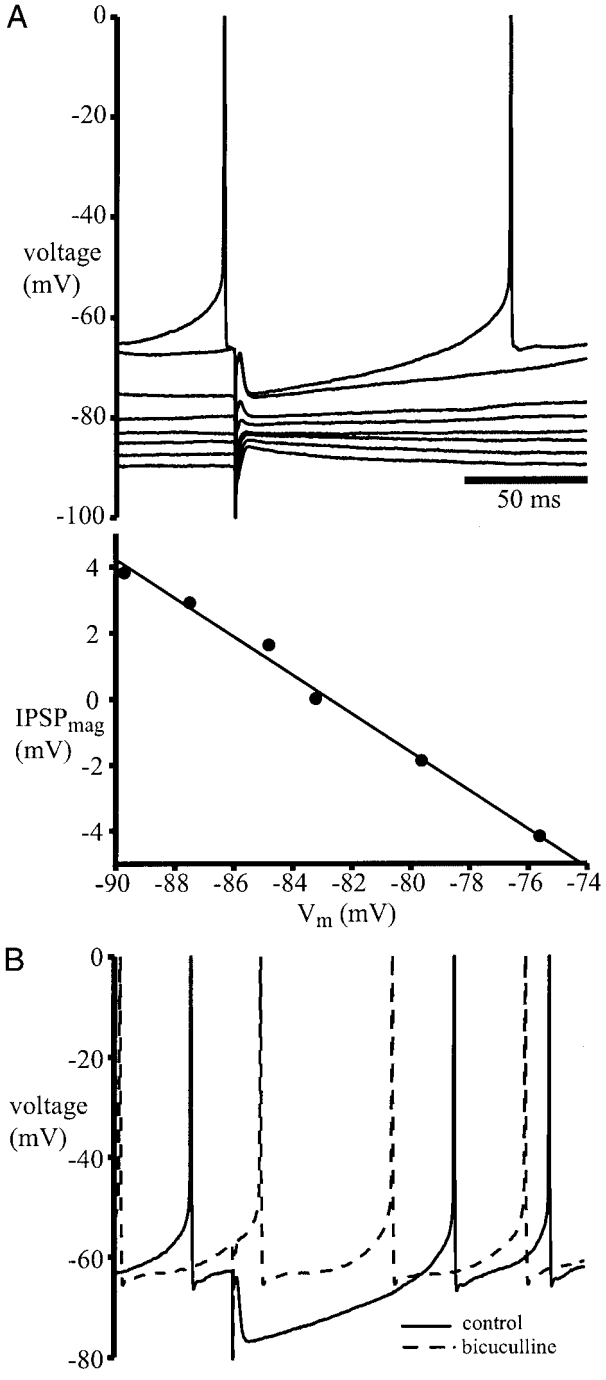

FIG. 1. Equilibrium potential of GABA-A inhibitory postsynaptic potentials (IPSPs) in subthalamic nucleus (STN) neurons. *A*: perforated-patch recording of a STN neuron. The membrane potential of the STN neuron was varied by constant current injection and an IPSP was evoked by electrical stimulation of the internal capsule (apparent vertical voltage deviation prior to the IPSP is an artifact of stimulation). In this and all subsequent figures, action potentials have been truncated at 0 mV for clarity. A graph of V_m against $IPSP_{mag}$ (plotted using the 6 most hyperpolarized values of V_m) demonstrates that, in this neuron, EGABA-A IPSP was approximately −83 mV (slope −0.58, $R = -1.0$, $n = 6$, $P < 0.0001$). *B*: the IPSP was entirely due to the synaptic activation of the GABA-A receptor because it was abolished completely by the bath application of the selective GABA-A antagonist bicuculline. Scale bar in *A* also applies to *B*.

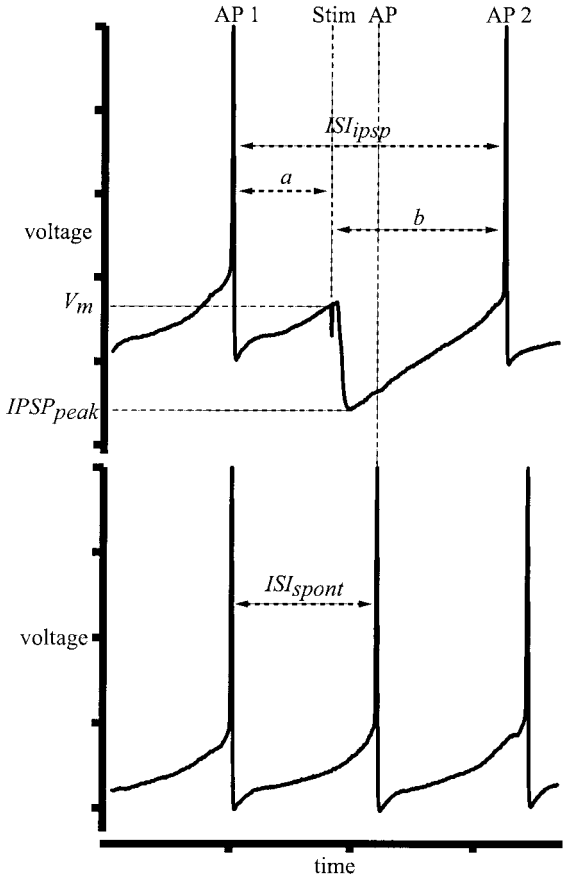

$$\text{phase} = a / \overline{ISI}_{spont}$$

$$IPSP_{mag} = IPSP_{peak} - V_m$$

FIG. 2. Schematic diagram detailing the measurement of GABA-A IPSPs and their effects on spontaneous action potential generation in STN neurons. GABA-A IPSPs were evoked in STN neurons at various points in the spontaneous oscillatory cycle that underlies the rhythmic generation of spikes by electrical stimulation of the internal capsule. The membrane potential at which the IPSP was evoked (V_m) was defined as the membrane potential immediately prior to the stimulation artifact (Stim). The time from the generation of the action potential immediately prior to the IPSP (AP1), to the onset of the electrical stimulation artifact was measured (*a*). The time from the onset of the electrical stimulation artifact to the generation of the action potential following the IPSP (AP2) was also measured (*b*). The time from AP1 to AP2 is equal to the interspike interval associated with the IPSP (ISI_{ipsp}). *B*: the phase of the oscillatory cycle of the postsynaptic STN neuron at which the IPSP was evoked was calculated from *a* divided by the average of the interspike intervals associated with spontaneous activity (ISI_{spont}). The magnitude of the IPSP ($IPSP_{mag}$) was calculated by subtracting V_m from the peak of the IPSP ($IPSP_{peak}$).

The ability of GABA-A IPSPs to drive the membrane potential to a narrow range of values (defined by the range of $IPSP_{peak}$) and the phase dependence of ISI_{ipsp} were related significantly to $IPSP_{mag}$ (Fig. 3). The phase dependence of ISI_{ipsp} was not related to the frequency of the oscillation (data not shown, slope = 3.74, $R = 0.17$, $n = 12$, $P = 0.59$).

The difference in the magnitude of IPSPs during the oscillatory cycle may, in addition to changes in driving force for chloride, also result from changes in the apparent input resis-

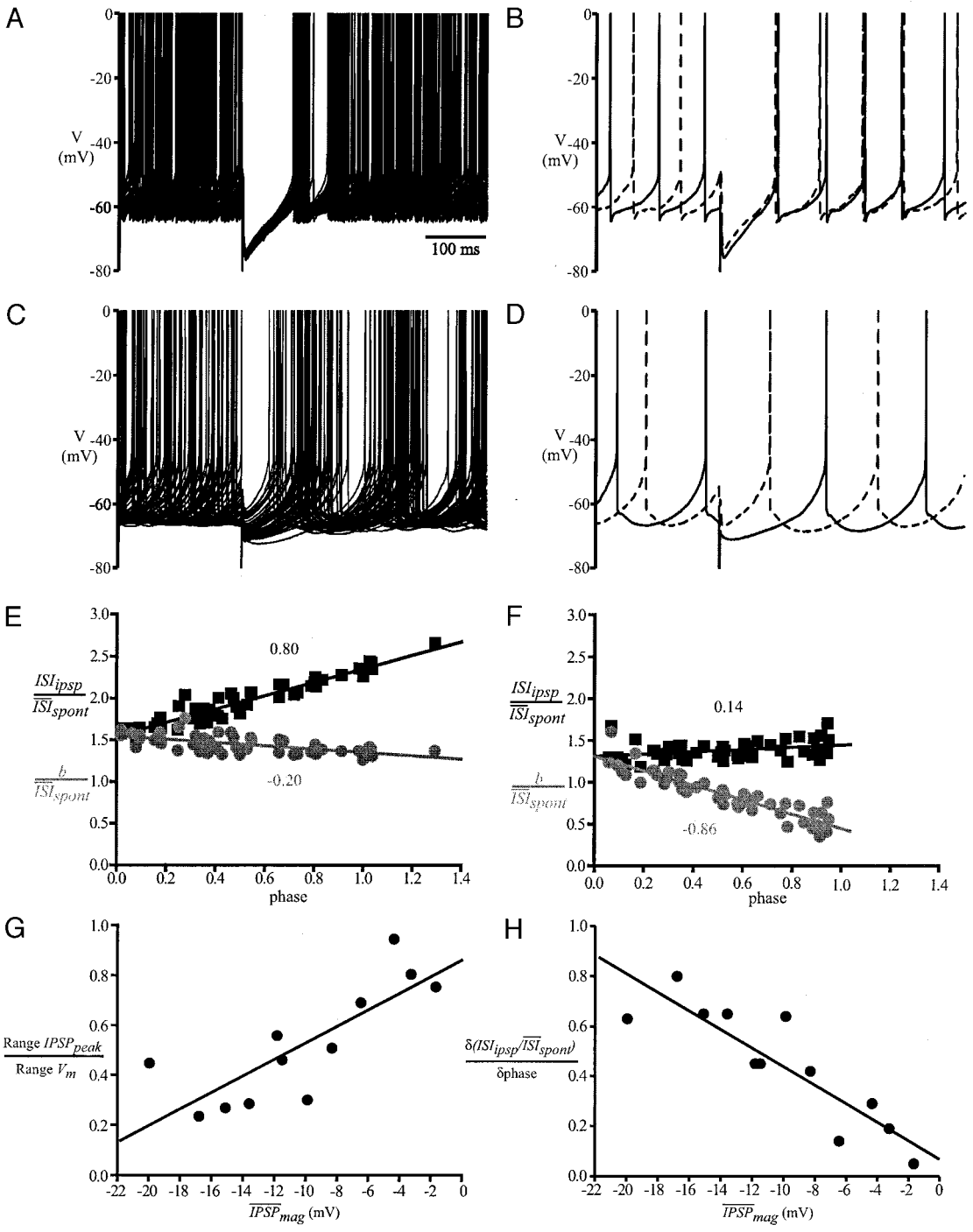

FIG. 3. The phase dependence of ISI_{ipsp} and b were related linearly to $IPSP_{mag}$ in STN neurons. *A*, *B*, and *E*: effect of a relatively large GABA-A IPSP (mean $IPSP_{mag}$ over 50 trials = −16.8 mV) on the timing of action potential generation in a STN neuron. Fifty superimposed sweeps (*A*) and 2 superimposed sweeps (*B*) are shown to demonstrate the resetting of the oscillation by the IPSP. *B*: note for 2 superimposed representative sweeps that action potential generation before the IPSP was completely out of phase, whereas action potential generation following the IPSP was almost exactly in phase. *C*, *D*, and *F*: effect of a relatively small GABA-A IPSP (mean $IPSP_{mag}$ over 50 trials = −6.5 mV) on the spontaneous activity of another STN neuron. Fifty superimposed sweeps (*C*) and 2 superimposed sweeps (*D*) are shown to demonstrate the failure of small IPSPs to reset consistently the oscillatory cycle. *D*: note for the 2 superimposed representative sweeps that action potential generation before the IPSP was partially out of phase and action potential generation following the IPSP was almost completely out of phase. *E*: for the neuron in *A* and *B* in which the evoked IPSPs were relatively large, there was a steep dependence of ISI_{ipsp} on the phase of the oscillation at which the IPSP was evoked (slope = 0.8, $R = 0.95$, $n = 50$, $P < 0.0001$), and the time to the action potential following the IPSP (b) was similar regardless of the phase at which the IPSP was evoked (slope = −0.2, $R = -0.59$, $n = 50$, $P < 0.001$). *F*: for the neuron in *C* and *D*, in which the evoked IPSP was relatively small, there was a relatively weak phase dependence of ISI_{ipsp} (slope = 0.14, $R = 0.33$, $n = 50$; $P = 0.02$) and a relatively steep negative phase dependence of b (slope = −0.86, $R = -0.91$, $n = 50$, $P < 0.0001$). In *E* and *F*, ISI_{ipsp} was normalized to the mean of ISI_{spont} to facilitate comparison of the effects of large and small IPSPs. *G*: the ratio of the range of $IPSP_{peak}$ to the range of V_m was related linearly to the mean $IPSP_{mag}$ (slope = 0.03, $R = 0.8$, $n = 12$, $P < 0.0018$). *H*: the dependence of ISI_{ipsp} on the phase of the oscillation at which the IPSP was evoked [$\delta(ISI_{ipsp}$/mean $ISI_{spont})/\delta$ phase] was related linearly to the mean $IPSP_{mag}$ (slope = −0.037, $R = -0.88$, $n = 12$, $P = 0.0001$). Calibration bar in *A* also applies to *B*–*D*.

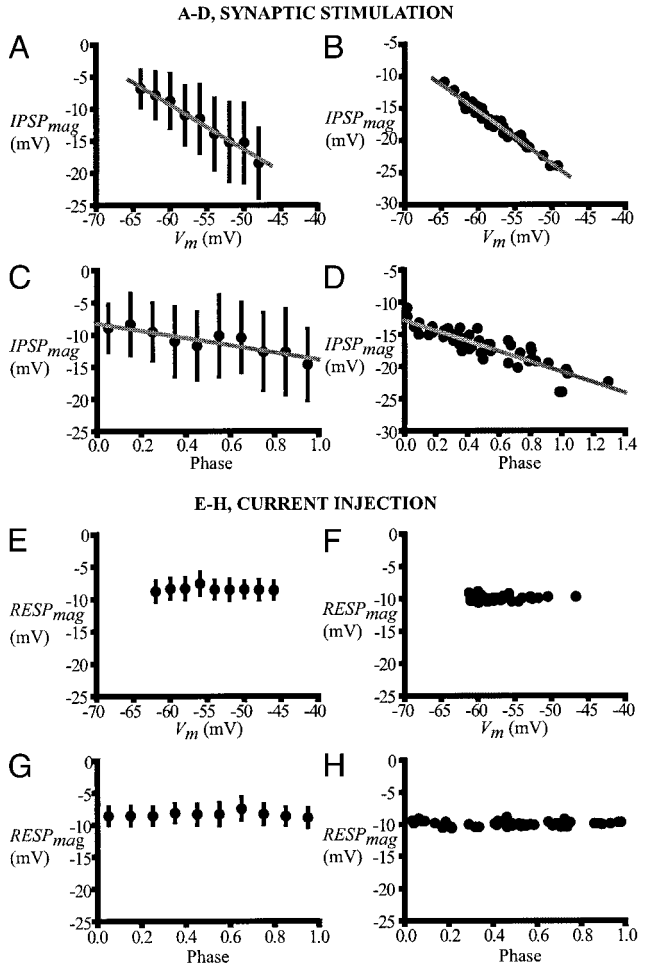

FIG. 4. $IPSP_{mag}$ was related linearly to V_m and phase within the voltage window traversed by the spontaneous oscillation. *A–D*: graphs of the mean voltage responses of 12 neurons (*A*, slope = −0.70, $R = -0.99$, $P < 0.0001$; *C*, slope = −5.58, $R = -0.9$, $P = 0.00034$) and a representative case (*B*, slope = −0.82, $R = -0.98$, $n = 50$ IPSPs, $P < 0.0001$; *D*, slope = −8.07, $R = -0.90$, $n = 50$ IPSPs, $P < 0.0001$) to synaptic stimulation, reveal the linear relationships between V_m and $IPSP_{mag}$, and between phase and $IPSP_{mag}$. *E–H*: graphs of the voltage responses of 5 neurons (*E*, slope = −0.01, $R = -0.15$, $P = 0.7$; *G*, slope = −0.01, $R = -0.01$, $P = 0.97$) and a representative neuron (*F*, slope = 0, $R = 0$, $n = 50$ responses, $P = 0.99$; *H*, slope = −0.17, $R = -0.12$, $n = 50$ responses, $P = 0.39$) to brief periods (10–20 ms) of hyperpolarizing current injection (50–100 pA) reveal no relationship between V_m and the voltage response to current injection ($RESP_{mag}$) or between phase and $RESP_{mag}$. Vertical bars in graphs *A*, *C*, *E*, and *G* are ±SD.

tance (Bennett and Wilson 1998) and/or active voltage-dependent amplification (Stuart 1999). To determine the factors influencing $IPSP_{mag}$ during the oscillatory cycle, we constructed graphs of V_m and phase against $IPSP_{mag}$ (Fig. 4, *A–D*) and the voltage response to brief periods of hyperpolarizing current injection (Fig. 4, *E–H*). These plots revealed that there was a linear increase in $IPSP_{mag}$ as the membrane potential depolarized during the oscillatory cycle (Fig. 4, *A–D*). In contrast, the magnitude of the voltage response to brief periods of hyperpolarizing current injection was similar within the voltage range of the oscillation and at different phases of the oscillatory cycle (Fig. 4, *E–H*). These data suggest that changes in driving force for chloride, the principal permeant ion of the GABA-A receptor, rather than changes in apparent input resistance or active voltage-dependent amplification, largely underlie the increase in $IPSP_{mag}$ during the oscillatory cycle.

Rebound burst firing properties of STN neurons and comparison of burst threshold with EGABA-A IPSP

The majority of STN neurons fired rebound bursts following the removal of hyperpolarizing current injection (Fig. 5; $n = 29$ of 31, 94%). The burst threshold in these neurons was −77.6 ± 4.7 mV, and the distribution of burst thresholds from this sample was not significantly different from a normal distribution (K-S test, $P = 0.84$). In the 29 neurons that fired rebound bursts, EGABA-A IPSP was −79.0 ± 7.0 mV and was equal to or more hyperpolarized than the burst threshold in 19 cases (65%). This result implies that GABA-A synaptic potentials are capable of producing sufficient hyperpolarization for the generation of rebound bursts in the majority of STN neurons. The duration of rebound burst activity in these 29 neurons was highly variable (compare Fig. 5, *A* with *B*). Current was applied for 500 ms to 25 of these neurons to generate peak hyperpolarizations (−79.5 ± 1.9 mV) that were similar to the mean EGABA-A IPSP (see above), and the durations of the rebound responses were recorded. The histogram of rebound burst duration was significantly different from a normal distribution (K-S test, $P = 0.037$), which implies that there may be more than one population of STN neurons with respect to the duration of their rebound bursts. Seventy-six percent of these neurons fired bursts of less than 100 ms duration (Fig. 5, *A1* and *A2;* $n = 19$; mean duration, 37.5 ± 23.9 ms). Twenty-four percent of these neurons fired bursts with durations greater than 100 ms (Fig. 5, *B1* and *B2;* $n = 6$; mean duration = 363.7 ± 286.5 ms). Both types of rebound burst activity were followed by the resumption of rhythmic single spike firing at lower frequency. These observations imply that the production of similar levels of hyperpolarization by GABA-A IPSPs may generate rebound burst responses in STN neurons, which are heterogeneous in nature and are partly dependent on the intrinsic burst-generating mechanisms in the postsynaptic neuron.

Multiple GABA-A IPSPs generate diverse patterns of activity in STN neurons

To determine the conditions necessary for the generation of rebound bursts, multiple GABA-A IPSPs were evoked at various frequencies and over different periods, and their impact was studied on 14 STN neurons held at different levels of polarization. Rebound burst firing was generated by multiple IPSPs in eight neurons (57%; Figs. 6–9). The amplitude of single IPSPs evoked at −70 mV, the EGABA-A IPSP and the burst threshold of neurons in which multiple IPSPs generated rebound burst firing ($IPSP_{mag}$ = −6.575 ± 2.7 mV; EGABA-A IPSP = −82.3 ± 2.7 mV; burst threshold = −74.9 ± 3.7 mV) were not significantly different ($IPSP_{mag}$ M-WU test, $P = 0.07$; EGABA-A IPSP M-WU test, $P = 0.053$; burst threshold M-WU test, $P = 0.11$) from neurons in which IPSPs failed to generate rebound burst firing ($IPSP_{mag}$ = −3.4 ± 2.6 mV; EGABA-A IPSP = −76.2 ± 5.2 mV; burst threshold = −80.8 ± 6.8 mV). In contrast, the difference between EGABA-A IPSP and burst threshold in neurons in which IPSPs generated rebound bursts (EGABA-A IPSP−burst

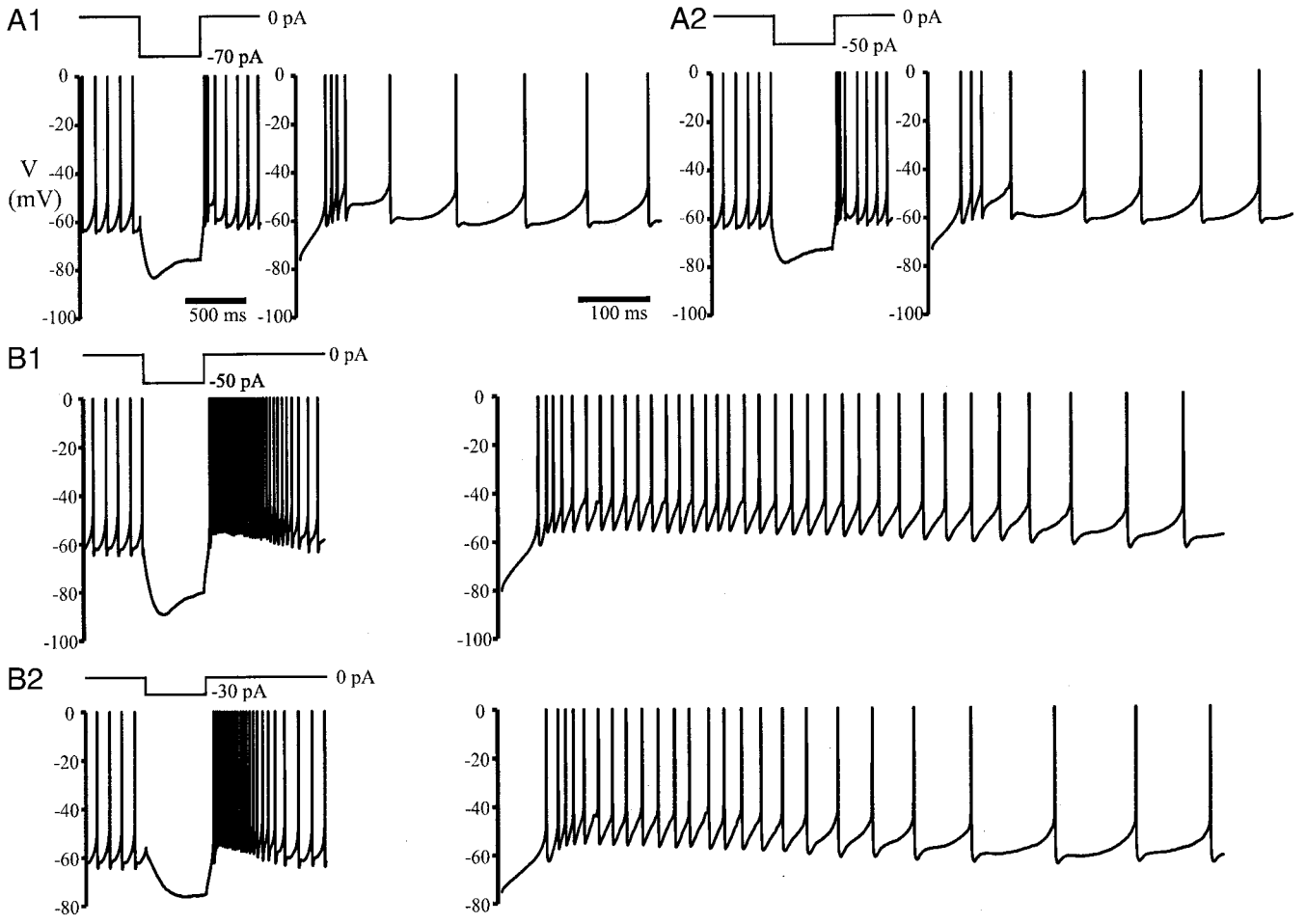

FIG. 5. STN neurons displayed heterogeneous rebound burst responses following the removal of hyperpolarizing current injection. *A1* and *A2*: the majority of STN neurons exhibited a short-lasting rebound burst, which was followed immediately by spontaneous rhythmic activity. The burst threshold of this example was −74.9 mV, and EGABA-A IPSP was −85 mV. The burst threshold and EGABA-A IPSP of this neuron implies that GABA-A IPSPs could produce sufficient hyperpolarization to generate a short-lasting rebound burst of activity. Note also that the frequency and number of action potentials generated within the burst were related to degree of hyperpolarization that was generated by current injection. *B1* and *B2*: approximately one quarter of STN neurons exhibited a long-lasting rebound response following the removal of hyperpolarizing current injection. Although this neuron was hyperpolarized to a similar degree to the example in *A1* and *A2*, the rebound burst responses were of much longer duration. The burst threshold of this example was −72.0 mV, and EGABA-A IPSP was −89.3 mV. These data imply that GABA-A IPSPs could produce sufficient hyperpolarization to generate a long-lasting rebound burst of activity. Note also that the frequency and number of action potentials generated within the burst and the duration of the burst were related to degree of hyperpolarization that was generated by current injection. Calibration bars and scales in *A1* apply to all panels.

threshold = −7.3 ± 3.2 mV) was significantly different (M-WU test, $P = 0.0019$) from neurons in which IPSPs failed to generate rebound bursts (EGABA-A IPSP–burst threshold = 4.6 ± 5.8 mV). Thus IPSPs that hyperpolarized STN neurons to membrane potentials equal to or more hyperpolarized than their burst thresholds generated rebound burst firing.

The interval between synaptic stimulation was fixed at 10 ms, and the number of IPSPs evoked was varied between 5 and 50 (Figs. 6–9). This pattern of synaptic stimulation was chosen to mimic synchronous high-frequency activity within the pallidosubthalamic pathway. This frequency of synaptic stimulation is within physiological limits because GP neurons may discharge at several hundred Hertz in vivo during normal and disordered movement [see the following reviews and papers referenced by Albin et al. (1989), Bergman et al. (1998), Chesselet and Delfs (1995), Crossman (1989), DeLong (1990), Levy et al. (1997), and Wichmann and DeLong (1996)] and in response to intracellular current injection (Cooper and Stanford 2000; Kita 1992; Nambu and Llinas 1994). As the number of IPSPs was increased, rebound bursts were generated from a wider range of polarization levels, and the intensity of the rebound burst evoked at each level of polarization was increased (Figs. 6–9). In neurons with short-duration rebounds ($n = 5$ of 8), increasing the number of IPSPs led to increases in the frequency of generation and the number of action potentials within a burst (e.g., Figs. 6*B* and 7). When rebound bursts were evoked, the duration of rebound activity was similar regardless of the number of IPSPs (Figs. 6*B* and 7). In neurons with longer duration rebound bursts ($n = 3$ of 8), increasing the number of IPSPs also led to an increase in the frequency and number of action potentials within a burst (Figs. 8*B* and 9). However, in these neurons the

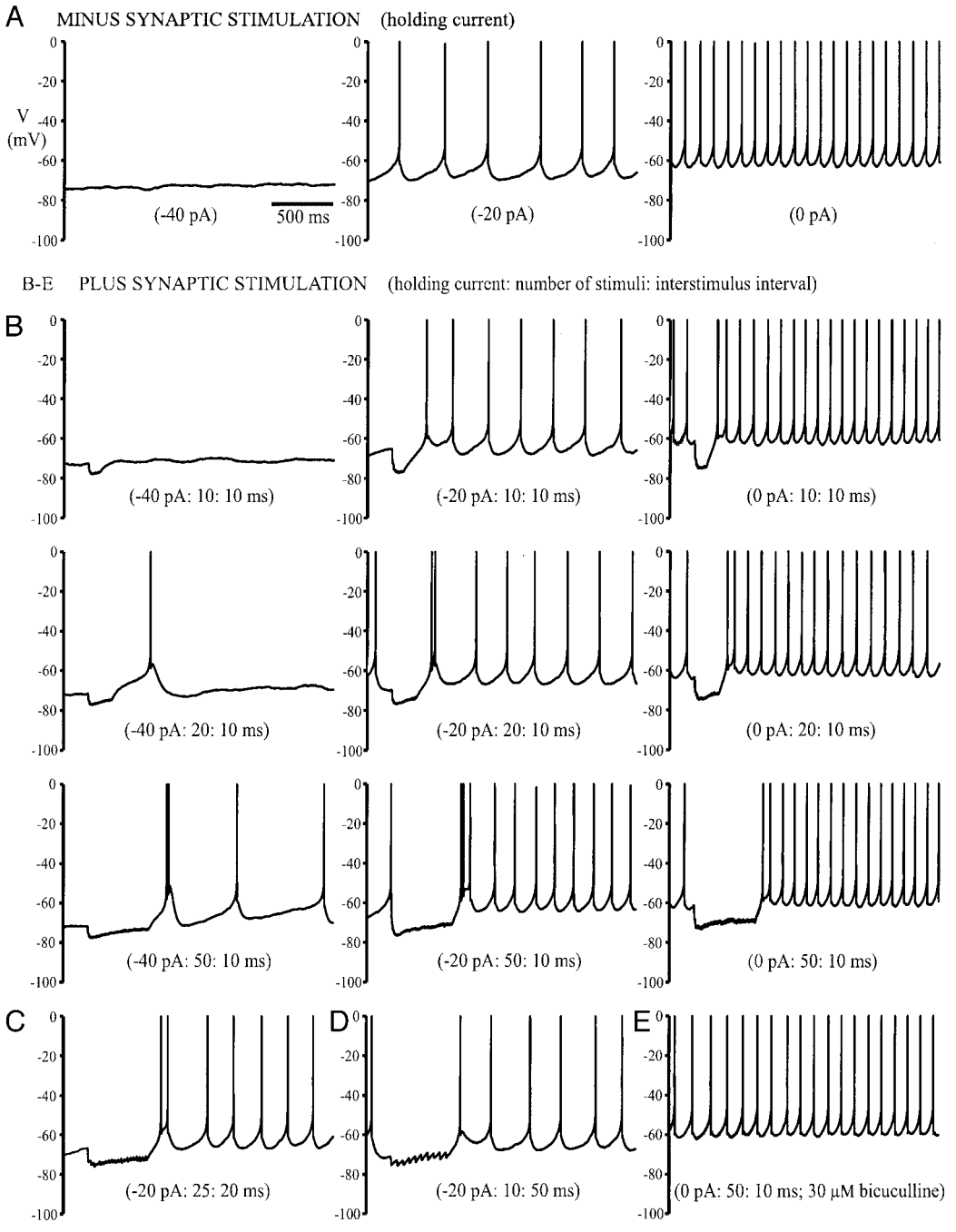

FIG. 6. Summation of GABA-A IPSPs produced sufficient hyperpolarization for the generation of short-duration rebound bursts in the majority of STN neurons. *A*: activity of a STN neuron during the constant injection of current (−40 or −20 pA) or in the absence of current injection. *B*: responses of the same STN neuron at various levels of polarization to 10, 20, and 50 GABA-A IPSPS stimulated at 10 ms intervals. With −40 pA holding current, 10 stimuli were not sufficient to generate a rebound burst, whereas 20 stimuli generated a single action potential, which rode on a broad underlying depolarization that was similar in form to a low-threshold calcium spike and 50 stimuli generated a rapid, but short-lasting rebound burst, which also appeared to ride on a low-threshold calcium spike. With −20 pA holding current, 10 stimuli generated a broad underlying depolarization, which was similar in form to a low-threshold calcium spike and on which rode a single action potential, 20 stimuli generated a short-duration rebound burst, and 50 stimuli generated a short-duration rebound burst of higher frequency. Note also that with −40 and −20 pA, the GABA-A IPSPs generated rhythmic spike generation after each rebound, that was of higher frequency than that generated with the same holding current in the absence of GABA-A IPSPs (*A*). Furthermore, the frequency of rhythmic action potential generation that followed the rebound burst response was related to the number of stimuli. With no holding current, 10, 20, and 50 stimuli generated only weak rebound responses. *B, C,* and *D*: with −20 pA holding current, delivery of stimuli at different rates over approximately 500 ms generated rebound responses and augmentations in rhythmic activity that were related to the frequency of stimulation. Thus stimulation at 10 ms intervals generated a rebound and augmentations in rhythmic activity, which were of the highest frequency, 20 ms intervals generated a rebound and rhythmic firing of lower frequency and 50 ms intervals generated an apparent low-threshold calcium spike on which only a single action potential was generated and the frequency of rhythmic firing after the burst was similar to that observed in the absence of IPSPs. *E*: IPSPs and responses of the STN neuron to synaptic stimulation were abolished completely by bath application of the selective GABA-A antagonist bicuculline (30 μM). Calibration bar and scale in *A* applies to all panels. Stimulation artifacts produced by multiple electrical stimulation have been removed from this and subsequent figures for clarity.

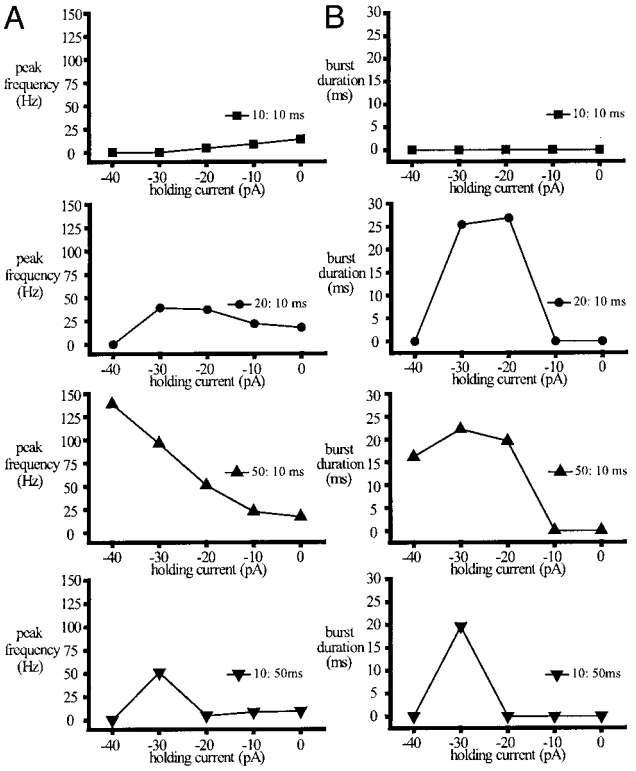

FIG. 7. The short-duration rebound burst response of STN neurons was a complex function of the pattern of presynaptic activity and the level of postsynaptic polarization. Multiple *X-Y* graphs generated from the neuron in Fig. 6 illustrating the relationships between the peak frequency of firing (*A*) and duration (*B*) of the burst response to various patterns of synaptic stimulation during the injection of a range of hyperpolarizing current. *A*: as the number of stimuli was increased and the interstimulus interval was held constant at 10 ms, the peak frequency of firing within the burst response increased, and burst responses were evoked from a wider range of polarization. When the period over which synaptic stimulation was carried out was kept similar (approximately 500 ms), the higher frequency of synaptic stimulation generated higher peak frequencies of firing within the burst response at each level of polarization (*A*), and burst responses were evoked from a wider range of polarization levels (*A* and *B*). *B*: the length of the short-duration rebound burst response was similar in each case and was not therefore related clearly to the pattern of synaptic input. *X*: *X* ms; number of stimuli: interstimulus interval.

duration of the rebound burst was related more clearly to the number of IPSPs (Figs. 8*B* and 9). The level of polarization that was associated with the rebound bursts of greatest intensity varied between neurons. In some neurons, the most intense burst was generated when the neuron was held close to or just below the threshold for rhythmic activity (e.g., Figs. 6 and 7). In other neurons, the most intense response was observed in the absence of holding current (e.g., Figs. 8 and 9).

Inhibitory postsynaptic potentials were also evoked over a period of approximately 500 ms, but the interval between IPSPs and the total number of IPSPs was varied. Intervals between 10 and 100 ms were chosen to mimic activity in the pallidosubthalamic pathway of between 10 and 100 Hz. As the frequency of synaptic stimulation was increased, rebound bursts were generated from more levels of polarization, and the intensity of the rebound burst, evoked at each level of polarization, was increased (Figs. 6–9). In neurons with short and longer duration rebound burst responses, increasing the frequency of synaptic stimulation led to an increase in the frequency of generation and number of action potentials within a burst (Figs. 6–9). When rebound bursts were evoked, the duration of rebound activity was related most clearly to the frequency of synaptic stimulation in neurons with longer duration rebounds (Figs. 8 and 9).

In addition to the generation of rebound bursts, multiple IPSPs influenced the activity of STN neurons in several other ways. Multiple IPSPs could evoke a single spike, which rode on a rebound depolarization that was similar in form to a low-threshold calcium spike (e.g., Fig. 6, *B* and *C*). In some cases, the rebound depolarization led to the restoration of rhythmic spiking activity, which was generally of a higher rate than that observed when the same level of holding current was applied and IPSPs were not evoked. Furthermore, the frequency of rhythmic spiking activity was related to the frequency and number of IPSPs that were evoked (Figs. 6 and 8). Sequences of IPSPs that failed to produce sufficient hyperpolarization for the generation of rebound activity or for the augmentation of rhythmic spiking simply reduced or abolished rhythmic spiking activity in STN neurons during the period in which they were evoked (Figs. 6 and 8). Multiple IPSPs and their influence on the spiking activity were abolished by the bath application of the selective GABA-A antagonist bicuculline ($n = 6$ of 6; Figs. 6*E* and 8*E*).

DISCUSSION

EGABA-A IPSP is more hyperpolarized than the voltage range associated with the spontaneous oscillation in STN neurons

Using perforated patch recording to maintain the natural regulation of intracellular anions, divalent cations, and larger molecules in the recorded neuron (Abe et al. 1994; Bevan et al. 2000; Kyrozis and Reichling 1995; Ulrich and Huguenard 1997), it was determined that the mean EGABA-A IPSP of STN neurons was -79.4 ± 7.0 mV. This value of EGABA-A IPSP suggests that if GABA-A current is dominant, then STN neurons will be hyperpolarized below the voltage range of the oscillation, to potentials associated with the complete deactivation of persistent sodium current, the activation of hyperpolarization activated cationic current, and the recovery from inactivation of low-threshold calcium current (Beurrier et al. 2000; Bevan and Wilson 1999; Nakanishi et al. 1987a; Song et al. 2000). The mechanisms underlying the maintenance of low concentrations of intracellular chloride that must be present for STN neurons to possess this relatively hyperpolarized value of EGABA-A IPSP are unknown, but the actions of the neuronal-specific potassium-chloride co-transporter (KCC2) may be important (Payne 1997).

Since GP neurons form GABAergic synapses with the somatic and dendritic membranes of STN neurons (Bevan et al. 1995, 1997; Smith et al. 1990), it is likely that GABA-A receptors were activated at synapses that were at variable distances from the somatic recording electrode. The membrane potential at the somatic recording site (V_m) is not necessarily equal to the membrane potential at the site(s) of the GABA-A receptor current, particularly if the site(s) of the current is (are) distal. Neurons are not uniform with respect to their passive and active membrane properties, and their responses to, and the

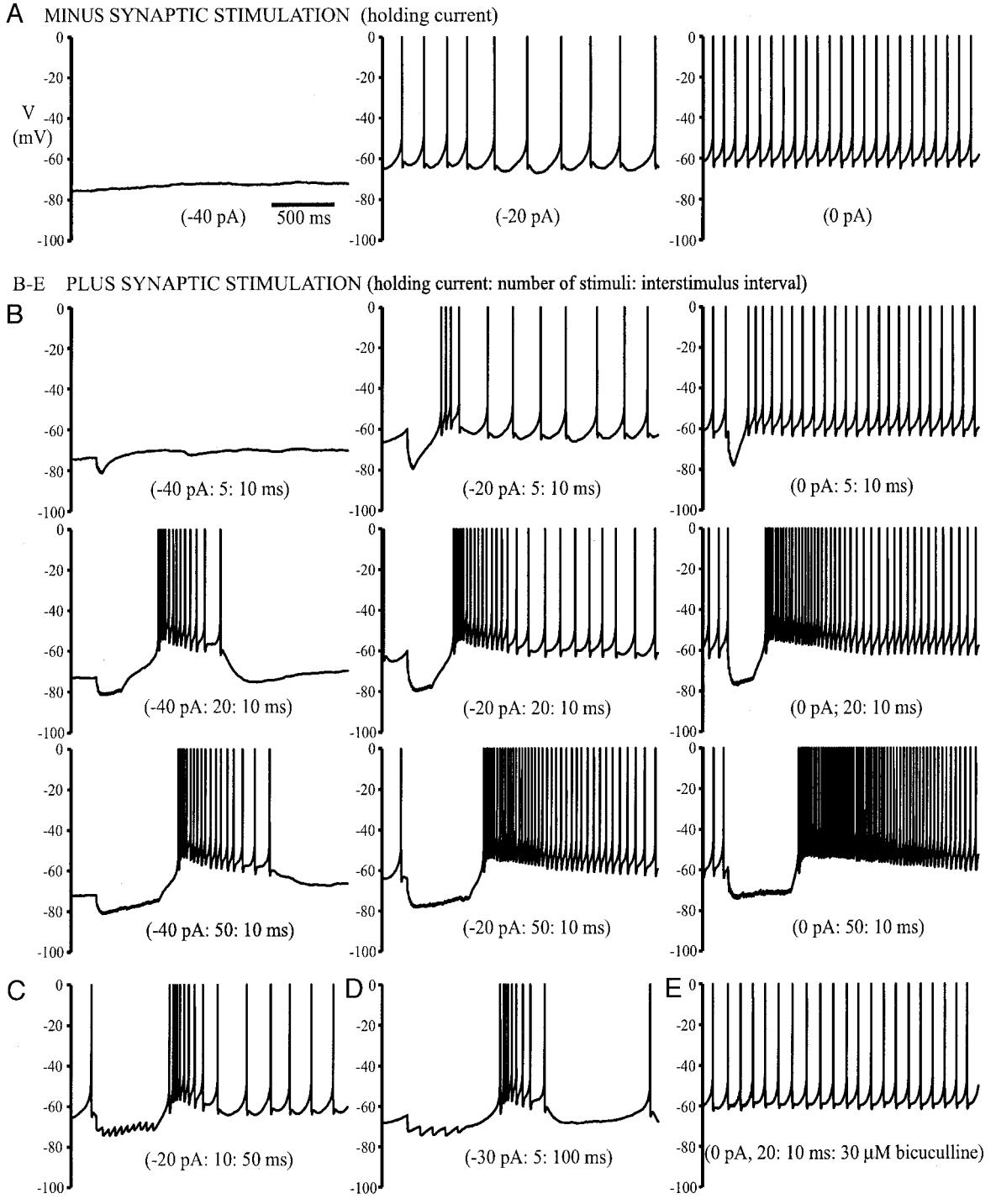

FIG. 8. Summation of GABA-A IPSPs produced sufficient hyperpolarization for the generation of long-duration rebound bursts in a minority of STN neurons. *A*: activity of a STN neuron during the constant injection of current (−40 or −20 pA) or in the absence of current injection. *B*: response of the same STN neuron held at various levels of polarization to 5, 20, and 50 GABA-A IPSPS stimulated at 10 ms intervals. With −40 pA holding current, 5 stimuli were not sufficient to generate rebound activity, whereas 20 stimuli generated a rebound burst and 50 stimuli generated a rebound burst of higher frequency and longer duration. With −20 pA holding current, 5, 20, and 50 stimuli generated rebound bursts of progressively greater frequency and duration. Note in each case that action potential firing throughout the sampling period was always of higher frequency than that generated with −20 pA holding current in the absence of GABA-A IPSPs (*A*). Furthermore, the frequency of rhythmic firing that followed the burst response was related to the number of stimuli. With no holding current, 5 stimuli were insufficient to generate a rebound burst, whereas 20 and 50 stimuli generated rebound bursts of progressively greater frequency and duration. *B* and *C*: with −20 pA holding current, stimulation at a different rate over approximately 500 ms generated rebound responses and augmentations in rhythmic activity that were related to the frequency of stimulation. Thus stimulation at 10 ms intervals generated a rebound burst that was of higher frequency and duration than that generated by stimulation at 50 ms intervals. *D*: a rebound burst was also generated using a very low rate of synaptic stimulation (100 ms interval) when a holding current of −30 pA was applied. A rebound burst could not be elicited at this low rate of stimulation when holding current of different magnitudes were applied, or in the absence of holding current. *E*: the IPSPs and responses of the STN neuron to synaptic stimulation were abolished completely by the bath application of the selective GABA-A antagonist bicuculline (30 μM). Calibration bar and scale in *A* applies to all panels.

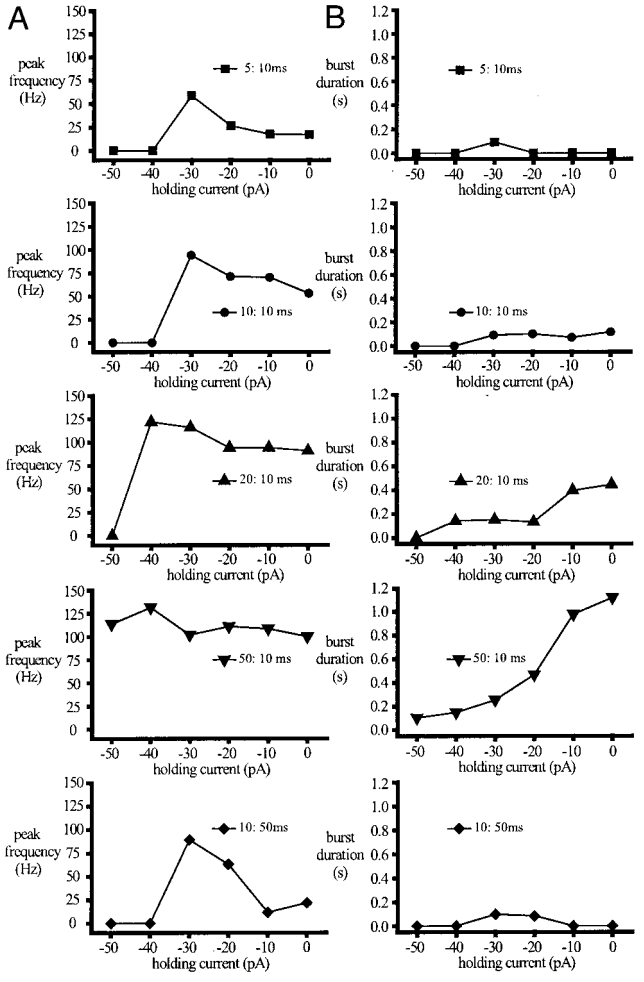

FIG. 9. The long-duration rebound burst response of STN neurons was a complex function of the pattern of presynaptic activity and the level of postsynaptic polarization. Multiple *X-Y* graphs generated from the neuron in Fig. 8 illustrating the relationships between the peak firing frequency (*A*) or duration (*B*) of the burst response to various patterns of synaptic stimulation during the injection of various levels of hyperpolarizing current. As the number of stimuli was increased and the interstimulus interval was held constant at 10 ms, the peak frequency of firing within rebound bursts (*A*) and the duration of burst responses increased (*B*), and burst responses were evoked from a wider range of polarization levels (*A* and *B*). When the period over which synaptic stimulation was carried out was kept similar (approximately 500 ms), the higher frequency of synaptic stimulation generated higher peak frequencies (*A*) and durations (*B*) of burst response for each level of polarization and burst responses were evoked from a wider range of polarization (*A* and *B*). Note the long duration of burst responses in this neuron, which were over 1 s in some cases. *X*: *X* ms; number of stimuli: interstimulus interval.

interaction of, holding and synaptic currents flowing at the soma or dendrites are difficult to predict [for comprehensive discussion of these issues see Hausser and Roth (1997) and the review by Spruston et al. (1994)]. Furthermore, neurons may regulate differentially the somatic and dendritic intracellular concentration of the permeant ions of the GABA-A receptor (Jarolimek et al. 1999). Despite these considerations, EGABA-A IPSP was similar to the equilibrium potential of GABA-A current that was determined by a technique that was not subject to such considerations, i.e., the pressure-pulse application of GABA close to the somatic site of recording (Bevan et al. 2000).

Phase dependence of the effect of single GABA-A IPSPs on the oscillation is related linearly to $IPSP_{mag}$ in STN neurons

Single GABA-A IPSPs evoked at various points in the oscillatory cycle had a spectrum of effects on ISI_{ipsp} and the timing of action potential generation following the IPSP. The largest IPSPs increased ISI_{ipsp} in a highly phase-dependent manner and almost completely reset the phase of the oscillation underlying rhythmic spiking. A current may, if it is sufficiently large, drive the membrane potential to the equilibrium potential of that current (reviewed by Hodgkin 1951). Thus the largest IPSPs produced phase resetting by driving the membrane potential to similar levels, close to EGABA-A IPSP, even though the membrane potential at which the IPSP was evoked varied considerably. Since EGABA-A IPSP was more hyperpolarized than the oscillation, the effect of large IPSPs was to drive the membrane potential below that associated with the oscillation and the activation of pacemaker persistent sodium current. The return of the membrane potential to voltages associated with the activation of persistent sodium current may be due simply to the passive decay of the IPSP and/or voltage-dependent currents, which briefly activate or recover from inactivation during the IPSP such as hyperpolarization-activated cationic current (Stuart 1999) and low-threshold calcium current, respectively. The largest IPSPs clearly disrupted the pacemaker mechanism because ISI_{ipsp} was often longer than two oscillatory cycles and *b* was often longer than a single oscillatory cycle. These data provide further evidence that the persistent sodium current, rather than calcium-activated potassium current, is the principal pacemaker of the oscillation (Beurrier et al. 2000; Bevan and Wilson 1999). Resetting of the oscillation would not have occurred if the oscillation period was set principally by the extrusion of calcium, which enters the intracellular compartment during action potentials (Bevan and Wilson 1999).

As IPSPs decreased in size, they produced more similar shifts in the phase of the oscillation and thus increased ISI_{ipsp} in a relatively phase-independent manner. The smallest GABA-A IPSPs did not produce sufficient hyperpolarization for the complete deactivation of persistent sodium current (Beurrier et al. 2000; Bevan and Wilson 1999), but rather reduced the level of activation and delayed the further activation of that current. Evidence that the smallest IPSPs delayed rather than reset the pacemaker mechanism comes from the observation that ISI_{ipsp} and *b* were typically shorter than two oscillatory cycles and a single oscillatory cycle, respectively.

Mathematical studies (Ermentrout 1996) predicted that single inhibitory inputs of moderate magnitude and duration would produce negative phase resetting curves (i.e., ISI_{ipsp} is always greater than ISI_{spont}) in type 1 excitable membranes (Hodgkin 1948) (display smooth transitions from quiescence to rhythmic activity). STN neurons are examples of neurons with type 1 membranes because they are capable of very low frequency ($<$0.1 Hz) rhythmic activity and thus display smooth transitions from quiescence to rhythmicity (Bevan and Wilson 1999). Thus in agreement with Ermentrout's prediction (Ermentrout 1996), ISI_{ipsp} was always greater than ISI_{spont}. Furthermore, rebound bursts or prolonged augmentations in activity were never observed following single GABA-A IPSPs. These observations indicate that respectively, low-threshold calcium current and hyperpolarization activated cationic cur-

rent were not deinactivated and activated sufficiently by single IPSPs to augment spiking activity relative to that observed in the absence of IPSPs.

The potentially complex interplay between GABA-A IPSP current and intrinsic currents (Bennett and Wilson 1998; Stuart 1999) does not appear to have a large differential effect on $IPSP_{mag}$ within the oscillatory cycle. Thus we observed a smooth increase in $IPSP_{mag}$ with V_m or phase. In contrast, the voltage response to brief periods of hyperpolarizing current injection was constant across the oscillatory cycle. These observations suggest that, within the voltage range of the oscillation, the variation in $IPSP_{mag}$ is dictated principally by the electrochemical gradient for chloride.

EGABA-A IPSP is equal to or more hyperpolarized than burst threshold in the majority of STN neurons; rebound burst responses of STN neurons are heterogeneous

The mean EGABA-A IPSP in STN neurons was more hyperpolarized than the potentials that previous studies have demonstrated are associated with the recovery from inactivation of low-threshold calcium current (Beurrier et al. 2000; Bevan and Wilson 1999; Bevan et al. 2000). Furthermore, EGABA-A IPSP was equal to or more hyperpolarized than the degree of hyperpolarization required for robust rebound burst firing responses in the majority of STN neurons. These observations suggest that GABA-A IPSPs may generate rebound burst firing in STN neurons.

In agreement with evidence from whole cell recordings (Beurrier et al. 1999; Song et al. 2000), we can confirm, with a recording technique that preserves natural calcium dynamics, that there is more than one population of STN neuron with respect to the duration of their rebound burst responses. Furthermore, short ($<$100 ms) and longer ($>$100 ms) duration rebound bursting behaviors appear to have distinct relationships to the degree of hyperpolarization produced by current injection. The frequency of generation and number of action potentials within a rebound burst are related to the magnitude of hyperpolarization in neurons with short and long duration rebounds. However, the duration of the rebound burst response is related most clearly to the degree of hyperpolarization in neurons with long duration rebounds. These data suggest that neurons with short and long duration rebounds might also respond to similar patterns of GABA-A synaptic inputs in a distinct manner.

Multiple GABA-A IPSPs generate a variety of firing patterns, including rebound bursts, in STN neurons

The present data demonstrate that multiple GABA-A IPSPs generate rebound bursts if the GABA-A IPSP is sufficiently large and the equilibrium potential of the IPSP is more hyperpolarized than the rebound burst threshold. When IPSPs were generated at 100 Hz and their number was increased from 5 to 50, the frequency of firing within a rebound burst increased, and rebound bursts were generated from a wider range of polarization levels. These observations indicate that summation of GABA-A IPSPs is required for the generation of rebound activity in STN neurons and that the rebound burst discharge of STN neurons is sensitive to the number of preceding IPSPs. Burst duration only increased with the number of IPSPs in neurons with long duration rebounds, confirming our hypothesis that the response of STN neurons to similar patterns of synaptic input depends to a large extent on intrinsic burst-generating mechanisms. When IPSPs were generated over approximately 500 ms and the frequency of synaptic stimulation was increased, the frequency of firing within a rebound burst was increased, and rebound bursts were evoked from a wider range of polarization levels. Thus the burst response of STN neurons also encodes the frequency of synaptic input. Burst duration also increased with the frequency of IPSP stimulation in neurons with long duration rebounds, providing further confirmation, that the responses of neurons with short and long duration rebounds to similar patterns of synaptic input are heterogeneous.

The level of polarization of STN neurons was critical in determining the impact of IPSPs and the nature of the response. When similar patterns of IPSPs were stimulated, the most intense burst responses could be observed when no holding current was applied or when neurons were held just below the threshold for firing. The optimum level of polarization for rebound burst responses to a given pattern of synaptic input is presumably a complex function of the relative states of activation and inactivation of the channels underlying rebound burst activity, which result from the combination of holding and synaptic currents. These data indicate that the pattern of synaptic input and the voltage of the postsynaptic neuron are critical determinants of rebound bursting activity. Similar relationships were demonstrated for unitary synaptic interactions between perigeniculate and lateral geniculate neurons (Kim et al. 1997).

Multiple GABA-A IPSPs also generated a single rebound spike, which could be followed by the restoration of rhythmic spiking activity. In these cases, the weaker activation of low-threshold calcium current associated with lower durations or rates of IPSP activity, is likely to be responsible for the generation of a single rebound spike. Although relatively weak, the rebound depolarization may be quite influential by causing sufficient depolarization for the subsequent activation of persistent sodium current and the restoration and/or augmentation of rhythmic spiking activity compared with activity in the absence of IPSPs.

In accordance with the more traditional role of GABA-A IPSPs in the inhibition of activity, multiple IPSPs could also generate hyperpolarization that was sufficient to disrupt or prevent rhythmic spiking activity but was not sufficient to generate rebound responses.

Functional implications

These data provide further evidence that GABAergic input from the GP is likely to exert a major influence on the rate and pattern of activity of STN neurons. Although single IPSPs invariably reduced firing frequency by delaying or resetting the oscillation underlying single spiking, multiple IPSPs could generate rebound burst activity. Summation of IPSPs was critical for the generation of rebound burst activity because this form of activity was never generated by single IPSPs and was sensitive to the degree of summation, which is a function of the frequency and number of IPSPs that were elicited. Critical determinants of the influence of GABAergic synaptic input on

STN neurons therefore include the magnitude, frequency, and number of IPSPs.

Before commenting on the wider functional significance of this study, it is important to note that several features of the study require such commentary to be treated as speculation. First, the study was carried out on slices from young rats. The properties of the recorded neurons were, however, similar to studies using more mature animals (Nakanishi et al. 1987a; Overton and Greenfield 1995). Second, the relevance of rodent data to human and nonhuman primates is unknown because the membrane properties of STN neurons in primates have not been studied. Third, since the slices used in this study were devoid of structured input from other STN afferents, the impact of GABAergic inputs may be more complex in vivo. In addition, the properties of STN neurons and GABAergic afferents in animals with intact dopamine systems may be different from those in dopamine-depleted animals. Finally, the proportion of GABAergic terminals that were stimulated electrically per STN neuron cannot be determined with the supramaximal stimulation technique applied in this study.

In resting animals, the majority of GP neurons display high rates of tonic activity, with occasional pauses in firing, and the activity of GP neurons are poorly correlated with each other (Bergman et al. 1998; DeLong et al. 1985; Nini et al. 1995; Raz et al. 2000; Turner and Anderson 1997; Urbain et al. 2000). Under these conditions, STN neurons discharge in a tonic-regular or -irregular fashion (Matsumara et al. 1992; Urbain et al. 2000; Wichmann et al. 1994). This and other recent studies suggest that tonic, poorly correlated synaptic input from the GP disrupts the oscillatory cycle and reduces the firing frequency of STN neurons but may not hyperpolarize STN neurons below the voltage range of the oscillation underlying spontaneous activity (Beurrier et al. 2000; Bevan and Wilson 1999; Bevan et al. 2000; Plenz and Kitai 1999; Song et al. 2000). Similar disruption of the output of neurons (that are rhythmically active in the absence of synaptic input) by synaptic input has been observed in other brain regions (Calvin and Stevens 1967, 1968; Gauck and Jaeger 2000; Hausser and Clark 1997; Stoop et al. 2000).

During movement, GP and STN neurons display more phasic, bursting patterns of activity (DeLong 1972; DeLong et al. 1985; Georgopoulos et al. 1983; Matsumara et al. 1992; Turner and Anderson 1997; Wichmann et al. 1994). During this behavior, the burst discharge of GP neurons may produce sufficient hyperpolarization of STN neurons for the recovery from inactivation of low-threshold calcium current. Rebound burst activity in STN neurons may then follow the end of the inhibitory burst. Another possibility is that synaptic input from cortical and/or thalamic afferents (Bevan et al. 1995; Fujimoto and Kita 1993; Kitai and Deniau 1981; Maurice et al. 1998; Mouroux et al. 1995; Smith et al. 1998) can generate burst activity in STN neurons with the involvement of low-threshold calcium current if they are active when STN neurons are hyperpolarized by the GP. When STN neurons are sufficiently depolarized for the complete inactivation of low-threshold calcium current, burst activity without the involvement of low-threshold calcium channels may also result from burst activity in cortical and thalamic afferents (Fujimoto and Kita 1993; Kitai and Deniau 1981; Magill et al. 2001; Maurice et al. 1998; Urbain et al. 2000).

In idiopathic and animal models of Parkinson's disease, GP and STN neurons display correlated rhythmic bursting activity (Bergman et al. 1994, 1998; Brown et al. 2001; DeLong 1990; Filion 1979; Gao et al. 1998; Krack et al. 1998; Levy et al. 2000; Magariños-Ascone et al. 2000; Magnin et al. 2000; Nini et al. 1995; Raz et al. 2000; Rodriguez et al. 1998). Under these conditions, STN neurons may receive rhythmic bursts of IPSPs that would summate sufficiently to lead to the rhythmic generation of rebound bursts in STN neurons. Since regions of the GP and STN are reciprocally connected (Shink et al. 1996; Smith et al. 1998), such activity may lead to the oscillation of the STN-GP network as rebound burst activity in STN neurons drives bursting in connected GP neurons, which in turn generate rebound activity in STN neurons and so on (Plenz and Kitai 1999). Whether this abnormal activity associated with Parkinson's disease is initiated within the STN-GP network (Plenz and Kitai 1999) or is a reflection of abnormal rhythmic bursting activity of afferents to this network (Magill et al. 2001) remains to be determined.

Interestingly, we also observed that the intrinsic properties of STN neurons are critical determinants of rebound bursting activity. Minute changes in the polarization of STN neurons were sufficient to alter the impact of similar patterns of IPSPs on STN neurons, suggesting that neuromodulators [e.g., acetylcholine (Féger et al. 1979), serotonin (Flores et al. 1995), and dopamine (Smith and Kieval 2000)] that are known to produce long-lasting changes in the polarization of neurons (reviewed by McCormick and Bal 1997) may be influential in determining the response of STN neurons to synaptic input from the GP. Finally, the observation that STN neurons are heterogeneous with respect to the duration of their rebound bursts implies that these neurons could participate in rhythmic burst activity of different frequencies. This view is consistent with the finding that STN neurons burst rhythmically at discrete frequencies within the 5- to 20-Hz band in idiopathic and animal models of Parkinson's disease (Bergman et al. 1994, 1998; Brown et al. 2001; DeLong 1990; Filion 1979; Krack et al. 1998; Levy et al. 2000; Magariños-Ascone et al. 2000; Magnin et al. 2000; Rodriguez et al. 1998).

Summary

Incoming GABAergic synaptic activity is encoded in a complex manner by STN neurons. Single IPSPs interact with the oscillatory cycle in a predictive manner that is related strongly to the $IPSP_{mag}$. In contrast, multiple IPSPs can produce sufficient hyperpolarization to generate rebound burst activity, the occurrence and nature of which is a function of the pattern of IPSPs and the membrane properties and voltage of the postsynaptic STN neuron.

The authors thank N. Kopell, J. Ritt, and D. Terman for comments on this study.

This research was supported by National Institute of Neurological Disorders and Stroke Grants NS-41280 (M. D. Bevan) and NS-24763 (C. J. Wilson) and the Medical Research Council, UK.

REFERENCES

ABE Y, FURUKAWA K, ITOYAMA Y, AND AKAIKE N. Glycine response in acutely dissociated ventromedial hypothalamic neuron of the rat: new approach with gramicidin perforated patch-clamp technique. *J Neurophysiol* 72: 1530–1537, 1994.

ALBIN RL, YOUNG AB, AND PENNY JB. The functional anatomy of basal ganglia disorders. *Trends Neurosci* 12: 366–375, 1989.

BENNETT BD AND WILSON CJ. Synaptic regulation of action potential timing in neostriatal cholinergic interneurons. *J Neurosci* 18: 8539–8549, 1998.

BERGMAN H, FEINGOLD A, NINI A, RAZ A, SLOVIN H, ABELES M, AND VAADIA E. Physiological aspects of information processing in the basal ganglia of normal and parkinsonian primates. *Trends Neurosci* 21: 32–38, 1998.

BERGMAN H, WICHMANN T, KARMON B, AND DELONG MR. The primate subthalamic nucleus. II. Neuronal activity in the MPTP model of parkinsonism. *J Neurophysiol* 72: 507–520, 1994.

BEURRIER C, BIOULAC B, AND HAMMOND C. Slowly inactivating sodium current (INaP) underlies single-spike activity in rat subthalamic neurons. *J Neurophysiol* 83: 1951–1957, 2000.

BEURRIER C, CONGAR P, BIOULAC B, AND HAMMOND C. Subthalamic neurons switch from single-spike activity to burst-firing mode. *J Neurosci* 19: 599–609, 1999.

BEVAN MD, CLARKE NP, AND BOLAM JP. Synaptic integration of functionally diverse pallidal information in the entopeduncular nucleus and subthalamic nucleus in the rat. *J Neurosci* 17: 308–324, 1997.

BEVAN MD, FRANCIS CM, AND BOLAM JP. The glutamate-enriched cortical and thalamic input to neurons in the subthalamic nucleus of the rat: convergence with GABA-positive terminals. *J Comp Neurol* 361: 491–511, 1995.

BEVAN MD AND WILSON CJ. Mechanisms underlying spontaneous oscillation and rhythmic firing in rat subthalamic neurons. *J Neurosci* 19: 7617–7628, 1999.

BEVAN MD, WILSON CJ, BOLAM JP, AND MAGILL PJ. Equilibrium potential of GABA-A current and implications for rebound burst firing in rat subthalamic neurons in vitro. *J Neurophysiol* 83: 3169–3172, 2000.

BROWN P, OLIVIERO A, MAZZONE P, INSOLA I, TONALI P, AND DI LAZZARO V. Dopamine dependency of oscillations between subthalamic nucleus and pallidum in Parkinson's disease. *J Neurosci* 21: 1033–1038, 2001.

BRUGGER F, WICKI U, OLPE HR, FROESTL W, AND MICKEL S. The action of new potent GABA-B receptor antagonists in the hemisected spinal cord preparation of the rat. *Eur J Pharmacol* 235: 153–155, 1993.

CALVIN WH AND STEVENS CF. Synaptic noise as a source of variability in the interval between action potentials. *Science* 155: 842–844, 1967.

CALVIN WH AND STEVENS CF. Synaptic noise and other sources of randomness in motoneuron interspike intervals. *J Neurophysiol* 31: 574–587, 1968.

CHESSELET MF AND DELFS JM. Basal ganglia and movement disorders. *Trends Neurosci* 19: 417–422, 1995.

COOPER AJ AND STANFORD IM. Electrophysiological and morphological characteristics of three subtypes of rat globus pallidus neurone in vitro. *J Physiol (Lond)* 527: 291–304, 2000.

CROSSMAN AR. Neural mechanisms in disorders of movement. *Comp Biochem Physiol A Physiol* 93: 141–149, 1989.

CURTIS DR, DUGGAN AW, FELIX D, AND JOHNSTON GA. Bicuculline and central GABA receptors. *Nature* 228: 676–677, 1970.

DELONG MR. Activity of basal ganglia neurons during movement. *Brain Res* 40: 127–135, 1972.

DELONG MR. Primate models of movement disorders of basal ganglia origin. *Trends Neurosci* 13: 281–285, 1990.

DELONG MR, CRUTCHER MD, AND GEORGOPOULOS AP. Primate globus pallidus and subthalamic nucleus: functional organization. *J Neurophysiol* 53: 530–543, 1985.

ERMENTROUT B. Type 1 membranes, phase resetting curves, and synchrony. *Neural Comput* 8: 979–1001, 1996.

FÉGER J, HAMMOND C, AND ROUZAIRE-DUBOIS B. Pharmacological properties of acetylcholine-induced excitation of subthalamic nucleus neurones. *Br J Pharmacol* 65: 511–515, 1979.

FILION M. Effects of interruption of the nigrostriatal pathway and of dopaminergic agents on the spontaneous activity of globus pallidus neurons in the awake monkey. *Brain Res* 178: 425–441, 1979.

FLORES G, ROSALES MG, HERNANDEZ S, SIERRA A, AND ACEVES J. 5-Hydroxytryptamine increases spontaneous activity of subthalamic neurons in the rat. *Neurosci Lett* 192: 17–20, 1995.

FUJIMOTO K AND KITA H. Response characteristics of subthalamic neurons to the stimulation of the sensorimotor cortex in the rat. *Brain Res* 609: 185–192, 1993.

GAO DM, BENAZZOUZ A, PIALLAT B, BRESSAND K, ILINSKY IA, KULTAS-ILINSKY K, AND BENABID AL. High-frequency stimulation of the subthalamic nucleus suppresses experimental resting tremor in monkey. *Neuroscience* 88: 201–212, 1998.

GAUCK V AND JAEGER D. The control of rate and timing of spikes in the deep cerebellar nuclei by inhibition. *J Neurosci* 20: 3006–3016, 2000.

GEORGOPOULOS AP, DELONG MR, AND CRUTCHER MD. Relations between parameters of step-tracking movements and single cell discharge in the globus pallidus and subthalamic nucleus of the behaving monkey. *J Neurosci* 3: 1586–1598, 1983.

HAUSSER M AND CLARK BA. Tonic synaptic inhibition modulates neuronal output pattern and spatiotemporal synaptic integration. *Neuron* 19: 665–678, 1997.

HAUSSER M AND ROTH A. Estimating the time course of the excitatory synaptic conductance in neocortical pyramidal cells using a novel voltage jump method. *J Neurosci* 17: 7606–7625, 1997.

HODGKIN AL. The local electrical changes associated with repetitive action in a nonmedullated axon. *J Physiol* 107: 165–181, 1948.

HODGKIN AL. The ionic basis of electrical activity in nerve and muscle. *Biol Rev* 26: 339–409, 1951.

JAROLIMEK W, LEWEN A, AND MISGELD U. A furosemide-sensitive K^+Cl^- cotransporter counteracts intracellular Cl^- accumulation and depletion in cultured rat midbrain neurons. *J Neurosci* 19: 4695–4704, 1999.

KIM U, SANCHEZ-VIVES MV, AND MCCORMICK DA. Functional dynamics of GABAergic inhibition. *Science* 278: 130–134, 1997.

KITA H. Responses of globus pallidus neurons to cortical stimulation: intracellular study in the rat. *Brain Res* 589: 84–90, 1992.

KITAI ST AND DENIAU JM. Cortical inputs to the subthalamus: intracellular analysis. *Brain Res* 214: 411–415, 1981.

KRACK P, BENAZZOUZ A, POLLAK P, LIMOUSIN P, PIALLAT B, HOFFMANN D, XIE J, AND BENABID AL. Treatment of tremor in Parkinson's disease by subthalamic nucleus stimulation. *Mov Disord* 13: 907–914, 1998.

KYROZIS A AND REICHLING DB. Perforated-patch recording with gramicidin avoids artifactual changes in intracellular chloride concentration. *J Neurosci Methods* 57: 27–35, 1995.

LEVY R, HAZRATI LN, HERRERO MT, VILA M, HASSANI OK, MOUROUX M, RUBERG M, ASENSI H, AGID Y, FÉGER J, OBESO JA, PARENT A, AND HIRSCH EC. Re-evaluation of the functional anatomy of the basal ganglia in normal and parkinsonian states. *Neuroscience* 76: 335–343, 1997.

LEVY R, HUTCHISON WD, LOZANO AM, AND DOSTROVSKY JO. High-frequency synchronization of neuronal activity in the subthalamic nucleus of parkinsonian patients with limb tremor. *J Neurosci* 20: 7766–7775, 2000.

MAGARIÑOS-ASCONE CM, FIGUEIRAS-MENDEZ R, RIVA-MEANA C, AND CÓRDOBA-FERNÁNDEZ A. Subthalamic neuron activity related to tremor and movement in Parkinson's disease. *Eur J Neurosci* 12: 2597–2607, 2000.

MAGILL PJ, BOLAM JP, AND BEVAN MD. Dopamine regulates the impact of the cerebral cortex on the subthalamic nucleus-globus pallidus network. *Neuroscience* 106: 313–330, 2001.

MAGNIN M, MOREL A, AND JEANMONOD D. Single-unit analysis of the pallidum, thalamus and subthalamic nucleus in parkinsonian patients. *Neuroscience* 96: 549–564, 2000.

MATSUMARA M, KOJIMA J, GARDNER TW, AND HIKOSAKA O. Visual and oculomotor functions of monkey subthalamic nucleus. *J Neurophysiol* 67: 1615–1632, 1992.

MAURICE N, DENIAU JM, GLOWINSKI J, AND THIERRY AM. Relationships between the prefrontal cortex and the basal ganglia in the rat: physiology of the corticosubthalamic circuits. *J Neurosci* 18: 9539–9546, 1998.

MCCORMICK DA AND BAL T. Sleep and arousal: thalamocortical mechanisms. *Annu Rev Neurosci* 20: 185–215, 1997.

MOUROUX M, HASSANI OK, AND FÉGER J. Electrophysiological study of the excitatory parafascicular projection to the subthalamic nucleus and evidence for IPSI- and contralateral controls. *Neuroscience* 67: 99–107, 1995.

NAKANISHI H, KITA H, AND KITAI ST. Electrical membrane properties of rat subthalamic neurons in an in vitro slice preparation. *Brain Res* 437: 35–44, 1987a.

NAKANISHI H, KITA H, AND KITAI ST. Intracellular study of rat substantia nigra pars reticulata neurons in an in vitro slice preparation: electrical membrane properties and response characteristics to subthalamic stimulation. *Brain Res* 437: 45–55, 1987b.

NAMBU A AND LLINAS R. Electrophysiology of globus pallidus neurons in vitro. *J Neurophysiol* 72: 1127–1139, 1994.

NERNST W. Zur Kinetik der in Losung befindlichen Korper: Theorie der Diffusion. *Z Phys Chem* 3: 613–637, 1888.

NINI A, FEINGOLD A, SLOVIN H, AND BERGMAN H. Neurons in the globus pallidus do not show correlated activity in the normal monkey, but phase-locked oscillations appear in the MPTP model of parkinsonism. *J Neurophysiol* 74: 1800–1805, 1995.

OVERTON PG AND GREENFIELD SA. Determinants of neuronal firing pattern in the guinea-pig subthalamic nucleus an in vivo and in vitro comparison. *J Neural Trans* 10: 41–54, 1995.

PAYNE JA. Functional characterization of the neuronal-specific K-Cl cotransporter: implications for $[K^+]_o$ regulation. *Am J Physiol Cell Physiol* 273: C1516–C1525, 1997.

PLENZ D AND KITAI ST. A basal ganglia pacemaker formed by the subthalamic nucleus and external globus pallidus. *Nature* 400: 677–682, 1999.

RAZ A, VAADIA E, AND BERGMAN H. Firing patterns and correlations of spontaneous discharge of pallidal neurons in the normal and the tremulous 1-methyl-4-phenyl-1,2,3,6-tetrahydropyridine vervet model of parkinsonism. *J Neurosci* 20: 8559–8571, 2000.

RINVIK E AND OTTERSEN OP. Terminals of subthalamonigral fibres are enriched with gluatamate-like immunoreactivity: an electron microscopic, immunogold analysis in the cat. *J Chem Neuroanat* 6: 19–30, 1993.

RODRIGUEZ MC, GURIDI OJ, ALVAREZ L, MEWES K, MACIAS R, VITEK J, DELONG MR, AND OBESO JA. The subthalamic nucleus and tremor in Parkinson's disease. *Mov Disord* 13: 111–118, 1998.

SHINK E, BEVAN MD, BOLAM JP, AND SMITH Y. The subthalamic nucleus and the external pallidum: two tightly interconnected structures that control the output of the basal ganglia in the monkey. *Neuroscience* 73: 335–357, 1996.

SMITH Y, BEVAN MD, SHINK E, AND BOLAM JP. Microcircuitry of the direct and indirect pathways of the basal ganglia. *Neuroscience* 86: 353–387, 1998.

SMITH Y, BOLAM JP, AND VON KROSIGK M. Topographical and synaptic organization of the GABA-containing pallidosubthalamic projection in the rat. *Eur J Neurosci* 2: 500–511, 1990.

SMITH Y AND KIEVAL JZ. Anatomy of the dopamine system in the basal ganglia. *Trends Neurosci* 23: S28–S33, 2000.

SMITH Y AND PARENT A. Neurons of the subthalamic nucleus in primates display glutamate but not GABA immunoreactivity. *Brain Res* 453: 353–356, 1988.

SONG W-J, BABA Y, OTSUKA T, AND MURAKAMI F. Characterization of Ca^{2+} channels in rat subthalamic nucleus neurons. *J Neurophysiol* 84: 2630–2637, 2000.

SPRUSTON N, JAFFE DB, AND JOHNSTON D. Dendritic attenuation of synaptic potentials and currents: the role of passive membrane properties. *Trends Neurosci* 17: 161–166, 1994.

STOOP R, SCHINDLER K, AND BUNIMOVICH LA. Neocortical networks of pyramidal neurons: from local locking and chaos to macroscopic chaos and synchronization. *Nonlinearity* 13: 1515–1529, 2000.

STUART G. Voltage-activated sodium channels amplify inhibition in neocortical pyramidal neurons. *Nature Neurosci* 2: 144–150, 1999.

STUART GJ, DODT HU, AND SAKMAN B. Patch-clamp recordings from the soma and dendrites of neurons in brain slices using infrared video microscopy. *Pflügers Arch* 423: 511–518, 1993.

TURNER RS AND ANDERSON ME. Pallidal discharge related to the kinematics of reaching movements in two dimensions. *J Neurophysiol* 77: 1051–1074, 1997.

ULRICH D AND HUGUENARD JR. Nucleus-specific chloride homeostasis in rat thalamus. *J Neurosci* 17: 2348–2354, 1997.

URBAIN N, GERVASONI D, SOULIÈRE F, LOBO L, RENTÉRO N, WINDELS F, ASTIER B, SAVASTA M, FORT P, RENAUD B, LUPPI PH, AND CHOUVET G. Unrelated course of subthalamic nucleus and globus pallidus neuronal activities across vigilance states in the rat. *Eur J Neurosci* 12: 3361–3374, 2000.

WATKINS JC. L-glutamate as a central neurotransmitter: looking back. *Biochem Soc Trans* 28: 297–309, 2000.

WICHMANN T, BERGMAN H, AND DELONG MR. The primate subthalamic nucleus. I. Functional properties in intact animals. *J Neurophysiol* 72: 494–506, 1994.

WICHMANN T AND DELONG MR. Functional and pathophysiological models of the basal ganglia. *Curr Opin Neurobiol* 6: 751–758, 1996.